Fabrication of Diamond/Cu Direct Bonding for Power Device Applications

Shinji Kanda[1], Yasuo Shimizu[2], Yutaka Ohno[3], Kenji Shirasaki[2], Yasuyoshi Nagai[2], Makoto Kasu[4], Naoteru Shigekawa[1], and Jianbo Liang[1*]

[1]*Electronic Information Systems, Osaka City University, 3-3-138 Sumiyoshi, Osaka 558-8585, Japan*

[2]*Institute for Materials Research (IMR), Tohoku University, 2145-2 Narita, Oarai, Ibaraki 311-1313, Japan*

[3]*Institute for Materials Research (IMR), Tohoku University, 2-1-1 Katahira, Sendai 980-8577, Japan*

[4]*Department of Electrical and Electronic Engineering, Saga University, 1 Honjo-machi, Saga 840-8502, Japan*

*E-mail: liang@osaka-cu.ac.jp

Direct bonding of diamond and Cu was successfully fabricated by surface activated bonding (SAB) method at room temperature. The interfacial structures of diamond/Cu bonding interface before and after annealing at 500 and 700 ℃ were investigated by transmission electron microscope (TEM) and electron energy-loss spectroscopy (EELS). A 4-nm-thick transition layer was formed at the bonding interface, the transition layer thickness decreased with annealing temperature. It was found that the atomic ratio of sp^2 bonding in the bonding interface was larger than that of the diamond separated from the bonding interface by approximately 50 nm, which indicated that the transition layer was composed of the amorphous or graphite and diamond. After annealing at 700 ℃, an intermediate layer of about 2 nm thick was observed at the bonding interface. There were no nanovoids and micro-cracks observed at the interface with annealing at temperature as high as 700 ℃. These results indicated that the diamond/Cu bonding interface has high thermal stability and can withstand the temperature rise of power devices during operating.

1. Introduction

Diamond has the highest thermal conductivity (22 W/cm · K) among materials and is the most potential material for suppressing the rise in the device temperature when integrated with electronic devices. Diamond is being explored as an efficient heat spreader substrate for GaN-based devices.[1,2] AlGaN/GaN high-electron mobility transitions (HEMTs) are commonly fabricated on SiC, sapphire, and Si substrates.[3-5] The thermal conductivities of SiC (4 W/cm · K), sapphire (0.5 W/cm · K), and Si (1.5 W/cm · K) are very low in comparison with that of diamond. The output power of the AlGaN/GaN HEMTs is limited by the thermal conductivity of the substrate materials. Because the heat generated by self-heating mainly transfers through the substrate, which would degrade devices performance and reliability.[6-8] It has been reported that AlGaN/GaN HEMTs grown on single crystal diamond (111) substrates by metalorganic vapor phase epitaxy obtained maximum drain current, cut-off frequency, and maximum oscillation frequency compared with that on SiC substrates.[9] The integration of GaN-based devices and diamond by direct growth and wafer bonding has been studied extensively in recent years, resulting in improved thermal management and three-fold increase in the devices output power.[10-12]

Devices are generally directly mounted onto the heat sink by solder bonding or hydrophilic bonding for devices module.[13,14] The thermal conductivities of the solder materials such as AgSn (0.33 W/cm · K) and AuSn (0.57 W/cm · K) are very low in comparison with those of heat sink materials Al (2.36 W/cm · K) and Cu (3.98 W/cm · K). A large thermal resistance exists between the device and the heat sink, which would be a significant thermal barrier for heat transfer from the device to the heat sink.[15] Furthermore, the solder bonding with an intermediate layer would significantly degrade the advantages of diamond used for heat spreader substrate. Direct bonding of diamond and Al or Cu is promising for heat transferring from the devices to the heat sink. It has been reported that the direct bonding of diamond and Al was achieved at room temperature by surface activated bonding (SAB) and obtained the high thermal stability of the bonding interface.[16] Cu is superior to Al in terms of heat dissipation because the thermal conductivity of Cu is higher than Al. We previously succeed in the fabrication of diamond and Cu direct bonding by SAB and obtained the bonding interface without nano-voids.[17] However, the structures of the bonding interface and the effects of the heating temperature on the bonding interface are still unknown, which are

necessary to have a better understanding of the nature of the bonding interface for designing the heat dissipation devices.

In this paper, we examine the structures of the diamond/Cu bonding interface and the effects of the heating temperature on the interfacial structure by transmission electron microscopy (TEM). The chemical bonding states of the bonding interface carbon atoms were investigated by electron energy loss spectroscopy (EELS). The thermal stability of the bonding interface was tested at annealing temperature as high as 700 ℃ in N_2 gas atmospheric.

2. Experimental methods

We used high-pressure, high-temperature (HPHT) synthetic (100) single-crystal diamond substrate and Cu plate for bonding experiments. The sizes of diamond and Cu are 4 mm × 4 mm × 0.5 mm and 10 mm × 10 mm × 0.25 mm, respectively. Diamond and Cu were cleaned with acetone and isopropyl alcohol in an ultrasonic bath for 300s, dried under N_2 flow, and then set in the chamber of SAB facilities. The surfaces of diamond and Cu were activated by the Ar fast atom beam (FAB) irradiation. After the surface activation, diamond and Cu were bonded to each other at room temperature by applying a pressure of 10 MPa, so that diamond/Cu direct bonding were fabricated by SAB.[18-21)] The structures of the diamond/Cu bonding interfaces was investigated using TEM (JEM-2200FS) equipped with an EELS apparatus. Carbon K-shell edge spectra were taken between 225 and 375 eV at an accelerating voltage of 200 kV by EELS. The nano-structural change of the bonding interface annealed at 500 and 700 ℃ were also investigated by TEM. The bonded samples were annealed separately at 500 and 700 ℃ for 5 min in N_2 gas ambient. The samples for transmission electron microscopy (TEM) observation were fabricated using focused ion beam (FIB) technique.

3. Results

The optical microscope image of the diamond/Cu bonded sample surface before annealing is shown in Fig.1. The bonded area of the bonding interface is visible from the image due to diamond is a transport material. Although a small unbonded region was observed on the upper left side of the bonded sample, an about 99 % area bonding of diamond and Cu was

achieved. This result indicated that the direct bonding of diamond and Cu could be formed at room temperature.

Figs. 2(a), 2(b), and 2(c) show a cross-sectional TEM image of the diamond/Cu bonding interface before annealing, the EELS spectra of the bonding interface and diamond separated from the bonding interface by approximately 50 nm, respectively. A transition layer was observed at the bonding interface, the transition layer thickness was estimated to be about 4 nm. No nano-voids or cracks were observed at the bonding interface, which indicated that the excellent bonding interface was obtained. The fitting of the EELS spectra was performed with a Gaussian function. As shown in Figs 2(a) and 2(b), the EELS spectra of the bonding interface and diamond were decomposed into 4 peaks located at 284.2, 290.8, 296.7, and 305.3 eV, which could be assigned to be π^*, σ_1^*, σ_2^*, and σ_3^* peaks, respectively. $\pi^*$and σ^* peaks are typical for the indicative sp^2 hybridized carbon in graphite or amorphous carbon and the tetrahedral coordination sp^3 carbon in diamond, respectively. By integrating the area of the decomposed peaks, the atomic ration of sp^2 is given by[22)]

$$sp^2(\%) = \frac{\pi^*/(\pi^*+\sigma^*)}{\pi^*_{graphite}/(\pi^*_{graphite}+\sigma^*_{graphite})} \qquad (1)$$

where $\pi^*_{graphite}$ and $\sigma^*_{graphite}$ are the percentages of sp^2 and sp^3 bonding in a standard graphite carbon. Here, sp^2 bonding was assumed to be approximately 95%.[23-25)] The atomic ratio of sp^2 bonding was calculated to be 8.1 and 1.3 % in the bonding interface and diamond separated from the bonding interface by approximately 50 nm, respectively.

The low magnification cross-sectional TEM images of the diamond/Cu bonding interface before and after annealing at 500 and 700 °C are shown in Figs. 3(a), 3(b), and 3(c), respectively. A straight line located in the center of the figures could be clearly recognized, which corresponds to the bonding interface of diamond and Cu. Note that there are two holes observed in the Fig. 3(c), which are induced by FIB irradiation during TEM sample fabrication process. A large amount of strain marks was observed on the Cu side of the bonding interface, which was caused in the manufacturing Cu plate process by the roller compression method. A pressure of 10 Mpa was applied during the bonding process, which is unlikely the cause of Cu strain. No cracks or micro voids were observed around the bonding interface before and after annealing at 500 °C. Even after annealing at temperature as high as 700 °C, the separation of the bonding interface was not observed.

Figs. 4(a), 4(b), and 4(c) show the high magnification cross-sectional TEM images of the diamond/Cu bonding interface before and after annealing at 500 and 700 ℃, respectively. A transition layer with a thickness of about 4 nm was observed the bonding interface before annealing. The transiton layer thickness was decreased to 2.5 nm after annealing at 500 °C. After annealing at 700 °C, no transition layer was observed at the bonding interface. The transition layer thickness highly depended on the post-annealing temperature, which thinned with annealing temperature. Instead of the transition layer, an intermediate layer with a thickness of about 1 nm was formed at the bonding interface. It is of paramount important that there are no nano-cracks or voids observed at the bonding interface as well as annealing at 700. These results suggest that the diamond/Cu bonding interface has high temperature stability over a wide treatment temperature range.

4. Discussion

It was found that there was a transition layer with a thickness of about 4 nm formed at the bonding interface before annealing (Fig. 2(a). Similar transition layers have also been reported for the Si/GaAs, GaAs/SiC, and Si/SiC bonding interface fabricated by SAB.[26-28] The transition layer was mainly due to the damaged layer formed by Ar beam irradiation during bonding process. The obtained atomic ratio value of sp^2 in the bonding interface was larger than that in the diamond separated from the bonding interface by approximately 50 nm, which corresponded to the portion decrease of the diamond and the portion increase of the amorphous or graphite carbons. These results were resulted from Ar beam irradiation process destroyed the diamond crystal structure during bonding process. It has been reported that the atomic ratio of sp^2 bonding increased in polycrystal diamond by ion bombardment.[29] The observed small atomic ratio of sp^2 bonding in the diamond should be related to the FIB irradiation during TEM sample fabrication process.

The transition layer thickness decreased with the annealing temperature increasing from room temperature to 500 °C. Furthermore, the transition layer disappeared from the bonding interface after annealing at 700 °C. These results indicated that the post-annealing process has impacts on the recovery of the damaged layer. According to our previous reports, the transition layer disappeared after annealing at high temperature, which were due to the recrystallization of the damaged layer.[28,30, 31] For the diamond/Si bonding interface, a SiC

intermediate layer was formed at the bonding interface after annealing at 1000 °C, which played a role of residual stress relaxation between diamond and Si.[31,32] Although, the thermal expansion coefficient of Cu (16.42×10^{-6}/K) is much larger than that of diamond (2.3×10^{-6}/K),[33] no any cracks or the separation of the bonding were observed at the diamond/Cu bonding interface even annealing at temperature as high as 700 °C. These results should be related to the structure change of the transition layer formed at the diamond/Cu bonding interface. The residual stress relaxation mechanism of the diamond/Cu bonding interface should be consistent with that of the diamond/Si bonding interface.[32] The intermediate layer formed at the bonding interface with annealing at 700 °C served as a role of relaxation layer. The intermediate layer should be caused by the interdiffusion of copper and carbon atoms. The crystal structure of the intermediate layer will be investigated as the next work.

It is true that the transition layer was formed at the diamond/Cu bonding interface, but the transition layer thickness was as thin as 4 nm, which is difficultly affected the thermal transfer across the bonding interface. Direct bonding of diamond and Cu is expected to reduce the thermal resistance between devices and heat sink. Minimum thermal resistance of the diamond/Cu bonding interface should be expected due to the absence of solder materials. Moreover, the diamond/Cu bonding interface has high temperature thermal stability as high as 700 °C, which indicated that the bonding interface could withstand the high temperature generated during power-devices operating.

5. Conclusions

We investigated the structures of the bonding interface with annealing at different temperatures and demonstrated the thermal stability of the diamond/Cu bonding interface. A transition layer was formed at the bonding interface, its thickness decreased as the annealing temperature increased. EELS measurements indicated that the peaks corresponded π*and σ* orbitals were observed in the EELS spectrum of the bonding interface and the amorphous or graphite carbon portion of the bonding interface was larger than that of the diamond separated from the bonding interface. After annealing at 700 °C, an intermediate layer was observed at the bonding interface. No micro-cracks and nano-voids were observed at the bonding interface before and after annealing at different temperatures. These results indicate

that the diamond/Cu bonding interface has high thermal stability and could be useful for connecting diamond and heat sink for high power devices.

Acknowledgments

This study was supported partly by Hirose International Scholarship Foundation and the Grant-in-Aid for Challenging Exploratory Research (18K19034) of the Ministry of Education, Culture, Sports, Science, and Technology (MEXT), Japan. The fabrication of TEM samples by FIB was performed at IMR (Oarai) under the Inter-University Cooperative Research Program in IMR (NO. 18M0045).

References

1) Y.Yamamoto, T.Imai, K.Tanabe, T.Tsuno, Y.Kumazawa, N.Fujimori, Diam. Relat. Mater. **6**, 1057 (1997).
2) K. Nosaeva, N. Weimann, M. Rudolph, W. John, O. Krueger and W. Heinrich, Electron. Lett. **51**, 1010 (2015).
3) Y.-F. Wu, D. Kapolnek, J. P. Ibbetson, P. Parikh, B. P. Keller, and U. K. Mishra, IEEE Trans. Electron Devices **48**, 2181 (2001).
4) V. Tilak, B. Green, V. Kaper, H. Kim, T. Prunty, J. Smart, J. Shealy, and L. Eastman, IEEE Electron Device Lett. **22**, 504 (2001).
5) Y.-F. Wu, A. Saxler, M. Moore, R. P. Smith, S. Sheppard, P. M. Chavarkar, T. Wisleder, U. K. Mishra, and P. Parikh, IEEE Electron Device Lett. **25**, 117 (2004).
6) G. Meneghesso, G. Verzellesi, F. Danesin, F. Rampazzo, F. Zanon, A. Tazzoli, M. Meneghini, E. Zanoni, IEEE Trans. Device Mater. Reliab. **8**, 332 (2008).
7) R. Gaska, A. Osinsky, J. Yang, M.S. Shur, IEEE Electron Device Lett. **19**, 89 (1998).
8) A. Sarua, H. Ji, M. Kuball, M.J. Uren, T. Martin, K.P. Hilton, R.S. Balmer, IEEE Trans. Electron Devices **53**, 2438 (2006).
9) K. Hirama, Y. Taniyasu, M. Kasu, Appl. Phys. Lett. **98**, 162112 (2011).
10) H. Sun, R.B. Simon, J.W. Pomeroy, D. Francis, F. Faili, D.J. Twitchen, M. Kuball, Appl. Phys. Lett. **106**, 111906 (2015).
11) D. Francis, F. Faili, D. Babic, F. Ejeckam, A. Nurmikko, H. Maris, Diamond Relat. Mater. **19**, 1525 (2012).
12) J. W. Pomeroy, M. Bernardoni, D. C. Dumka, D. M. Fanning, M. Kuball, Appl. Phys. Lett. **104**, 083513 (2014).
13) M. Kuznetsov, F. Hakimi, R. Sprague, A. Mooradian, IEEE Photon. Technol. Lett. **9**, 1063 (1997).
14) Z.L. Liau, Appl. Phys. Lett. **77**, 651 (2000).
15) A. Saura, H.Ji, K.P. Hilton, D.J. Wallis, M.J. Uren, T. Martin, M. Kuball, IEEE Trans. Electron Devices **54**, 3152 (2007).
16) J. Liang, S. Yamajo, M. Kuball, N. Shigekawa, Scripta Mater. **159**, 58 (2019).
17) S. Kanda, S. Masuya, M. Kasu, N. Shigekawa, and J. Liang, Proc. 6th Int. IEEE Workshop Low-Temperature Bonding for 3D Integration, 2019, p. 57.

18) H. Takagi, K. Kikuchi, R. Maeda, T. R. Chung, and T. Suga, Appl. Phys. Lett. **68**, 2222 (1996).
19) J. Liang, T. Miyazaki, M. Morimoto, S. Nishida, N. Shigekawa, J. Appl. Phys. **114**, 183703 (2013).
20) T. H. Kim, M. M. R. Howlader, T. Itoh, T. Suga, J. Vac. Sci. & Technol. **21**, 449 (2003).
21) J. Liang, S. Masuya, M. Kasu, N. Shigekawa, Appl. Phys. Lett. **110**, 111603 (2017).
22) P. J. Fallon and L. M. Brown, Diamond Relt. Mater. **2**, 1004 (1993).
23) D. F. R. Mildner and J. M. Carpenter, J. Non-Cryst. Solids, **47**, 391 (1982).
24) C. Gao, Y. Y. Wand, A. L. Ritter, and J. R. Dennision, Phys. Rev. Lett. **62**, 954 (1989).
25) G. Galli, R. M. Martin, R. Car, and M. Parrinello, Phys. Rev. Lett. **62**, 555 (1989).
26) J. Liang, T. Miyazaki, M. Morimoto, S. Nishida, N. Watanabe, and N. Shigekawa, Appl. Phys. Express **6**, 021801 (2013).
27) E. Higurashi, K. Okumura, K. Nakasuji, and T. Suga, Jpn. J. Appl. Phys. **54**, 030207 (2015).
28) J. Liang, S. Nishida, M. Arai, and N. Shigekawa, Appl. Phys. Lett. **104**, 161604 (2014).
29) D. Bullutaud, N. Simon, H. Girard, E. Rzepka, and B. Bouchet-Fabre, Diamond Relat. Mater. **15**, 716 (2006).
30) S. Yamajo, S. Yoon, J. Liang, H. Sodabanlu, K. Watanabe, M. Sugiyama, A. Yasui, E. Ikenaga, and N. Shigekawa, Appl. Sur. Sci. **473**, 627 (2019).
31) J. Liang, S. Masuya, S. Kim, T. Oishi, M. Kasu, and N. Shigekawa, Appl. Phys. Express 12, 016501 (2019).
32) J. Liang, Y. Zhou, S. Masuya, F. Gucmann, M. Singh, J. Pomeroy, S. Kim, M. Kuball, M. Kasu, and N. Shigekawa, Diamond Relat. Mater. **93**, 187 (2019).
33) K. Yoshida and H. Morigami, Microelectronics Reliability **44**, 303 (2004).

Figure Captions

Fig. 1. The optical microscope image of the diamond/Cu bonded sample surface without annealing.

Fig. 2. A cross-sectional TEM image of the diamond/Cu bonding before annealing (a), EELS spectra of the bonding interface (b) and diamond separated from the bonding interface by approximately 50 nm (c).

Fig. 3. Low magnification cross-sectional TEM images of the diamond/Cu bonding interfaces before (a) and after annealing at 500 (b) and 700 ℃ (b).

Fig. 4. High magnification cross-sectional TEM images of the diamond/Cu bonding interface before (a) and after annealing at 500 (b) and 700 ℃ (b).

Figures

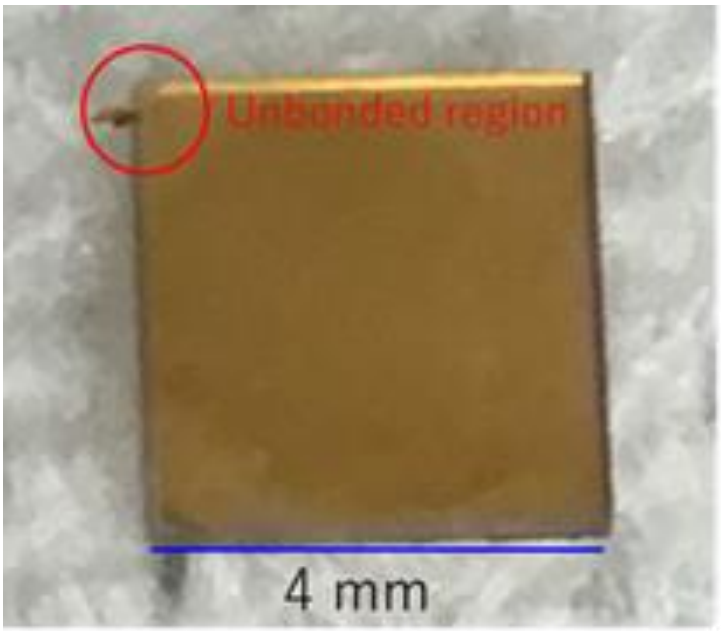

Fig. 1. Shinji Kanda et al.

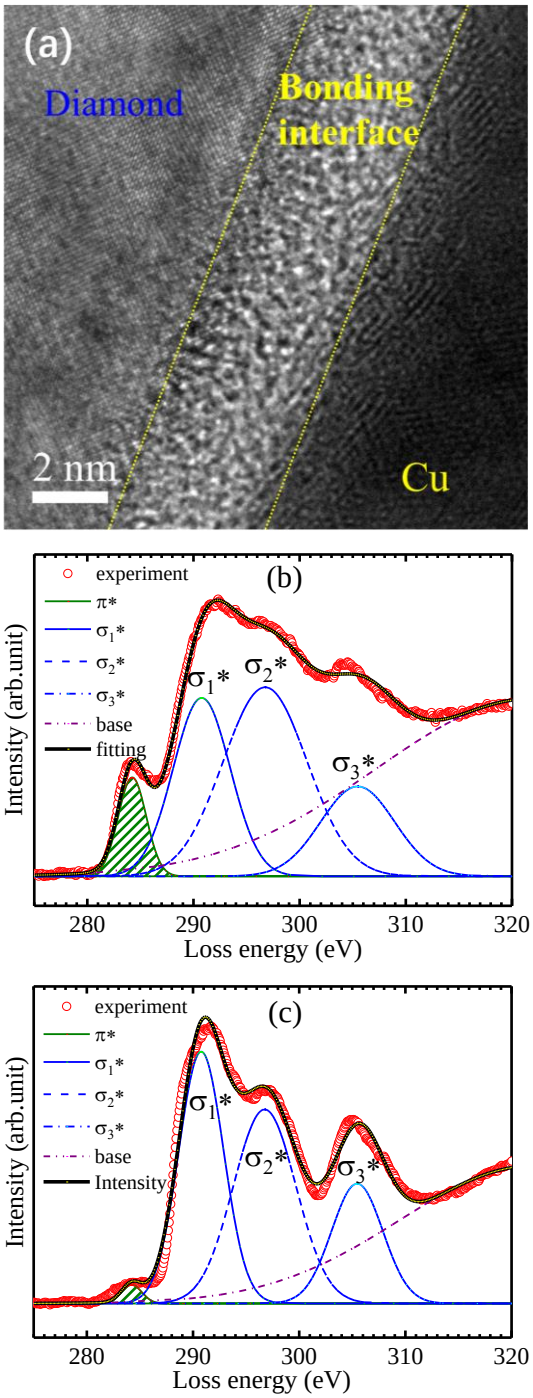

Fig. 2. 2(a),2(b). Shinji Kanda et al.

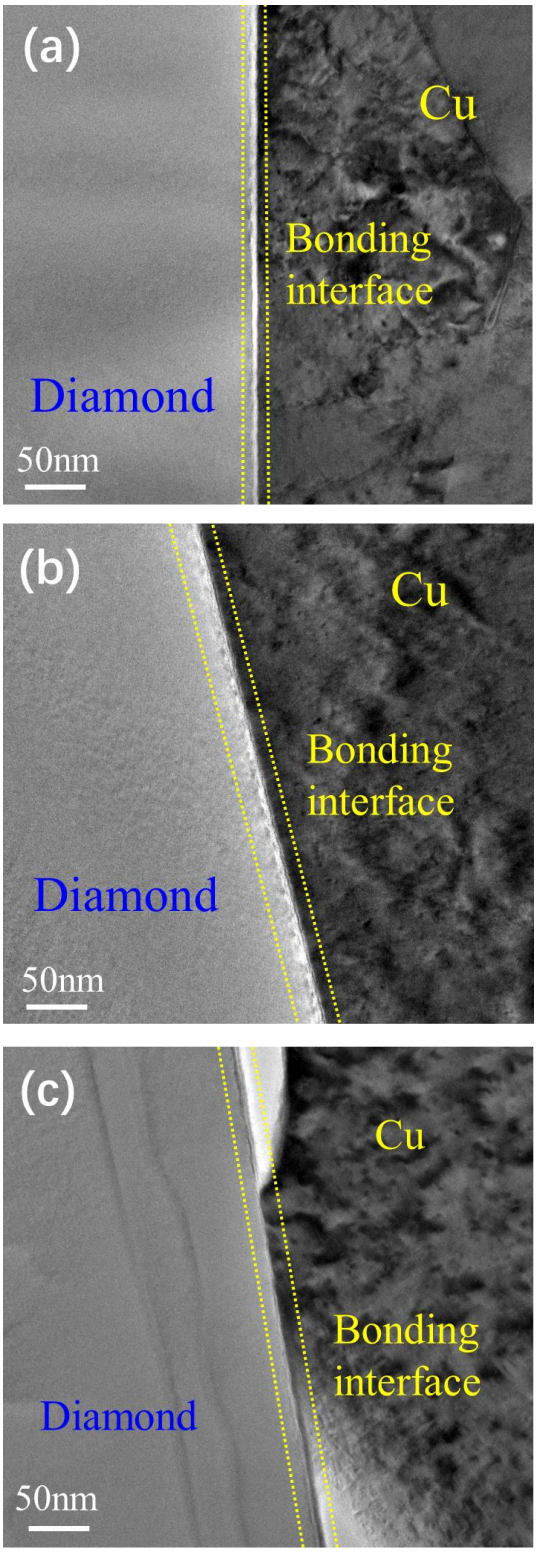

Figs. 3(a), 3(b), and 3(c) Shinji Kanda et. al.

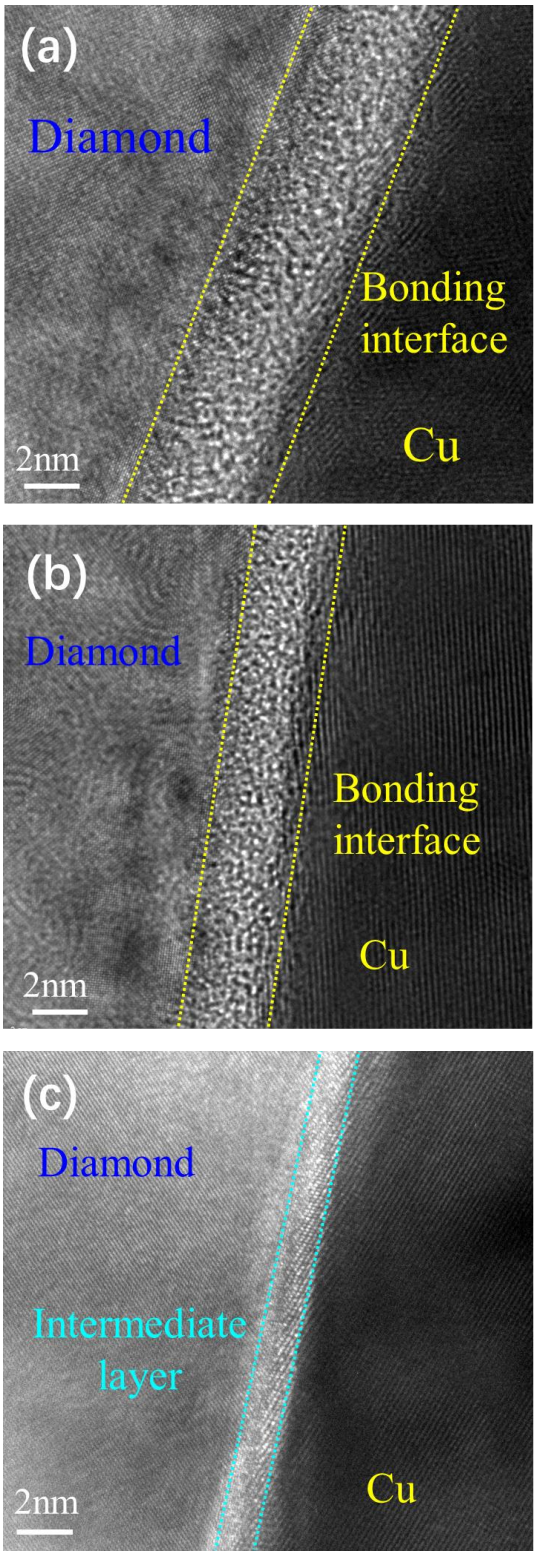

Figs. 4(a), 4(b), and 4(c) Shinji Kanda et al.